Acta Oceanol. Sin., 2020, Vol. 39, No. 2, P. 107–122
https://doi.org/10.1007/s13131-020-1545-9
http://www.hyxb.org.cn
E-mail: hyxbe@263.net

Specific oceanographic characteristics and phytoplankton responses influencing the primary production around the Ulleung Basin area in spring

Minji Lee[1], Jin Ho Kim[1], Yun-Bae Kim[2], Chan Hong Park[3], Kyoungsoon Shin[1], Seung Ho Baek[1]*

[1] South Sea Research Institute, Korea Institute of Ocean Science and Technology, Geoje 53201, Korea

[2] Ulleungdo/Dokdo Ocean Science Station, Korea Institute of Ocean Science and Technology, Ulleungdo 40205, Korea

[3] Dokdo Research Center, East Sea Research Institute, Korea Institute of Ocean Science and Technology, Uljin 36315, Korea

Received 26 October 2018; accepted 12 December 2018

Abstract

The East Sea (Sea of Japan) is a marginal, semi-closed sea in the northwestern Pacific. The Ulleung Basin area, which is located near the subpolar front of the East Sea, is known to have high primary production and good fisheries in spring season. After episodic wind-driven events during the spring of 2017, horizontal and vertical profiles of physical chemical biological factors were investigated at 29 stations located in the Ulleung Basin area. In addition, growth responses of phytoplankton communities to nutrient additions were evaluated by bioassay experiments to understand the fluctuation of phytoplankton biomass. Because of strong northwestern wind, phytoplankton biomass was scattered and upwelling phenomenon might be suppressed in this season. The phytoplankton abundances in the coastal stations were significantly higher than offshore and island stations. In contrast, the nutrient and chlorophyll *a* (Chl *a*) concentrations and the phytoplankton biomass were quite low in all locations. Bacillariophyceae was dominated group (>75.1% for coastal, 40.0% for offshore and 43.6% for island stations). In the algal bioassays, the phytoplankton production was stimulated by N availability. The *in vivo* Chl *a* values in the +N and +NP treatments were significantly higher than the values in the control and the +P treatments. Based on the field survey, the higher nutrients in coastal waters affected the growth of diatom assemblages, however, little prosperity of phytoplankton was observed in the offshore waters despite the injection of sufficient nutrients in bioassay experiments. The growth of phytoplankton depended on the initial cell density. All of results indicated that a dominant northwestern wind led to a limited nutrients condition at euphotic layers, and the low level of biomass supply from the coasts resulted in low primary production. Both supplying nutrients and introducing phytoplankton through the currents are critical to maintain the high productivity in the Ulleung Basin area of the East Sea.

Key words: Ulleung Basin, Ulleungdo and Dokdo, spring phytoplankton blooms, episodic windstorm, algal bioassays, primary production

Citation: Lee Minji, Kim Jin Ho, Kim Yun-Bae, Park Chan Hong, Shin Kyoungsoon, Baek Seung Ho. 2020. Specific oceanographic characteristics and phytoplankton responses influencing the primary production around the Ulleung Basin area in spring. Acta Oceanologica Sinica, 39(2): 107–122, doi: 10.1007/s13131-020-1545-9

1 Introduction

The East Sea (Sea of Japan) is a marginal, semi-closed sea in the northwestern Pacific located between the Eurasian continent and Japan. The average water depth of the East Sea is 1 700 m, and this sea consists of three major basins: the Ulleung Basin to the southwest, the Yamato Basin to the south, and the Japan Basin to the north (Isobe and Isoda, 1997); these bases are deeper than 2 000 m. The East Sea is connected to the East China Sea, the North Pacific Ocean, and the Sea of Okhotsk through the Korea/Tsushima Strait (hereafter referred to as the Korea Strait: KS), the Tsugaru Strait (TS), the Soya Strait (SS), and the Tartar/Mamiya Strait (T/MS). The inflow is primarily from the KS in the southwest, and the outflow is primarily through the TS and the SS in the eastern East Sea (Ohshima, 1994; Martin and Kawase, 1998). As the water depths of these straits are less than 150 m, the water exchange between the East Sea and the North Pacific Ocean is limited, and the volume of water transported through the KS has a major impact on hydrography and circulation in the East Sea (Ohshima, 1994; Kim and Yoon, 1999). The East Sea has a well-defined subpolar front at approximately 37°–40°N (Isoda and Saitoh, 1993; Isobe and Isoda, 1997), which is adjacent to the East Korea Warm Current (EKWC) that branches from the Tsushima Warm Current through the KS; the cold waters originate from the north.

The Ulleung Basin, which is located near the subpolar front, is known to have high primary production and good fisheries

Foundation item: The Basic Core Technology Development Program for the Oceans and the Polar Regions of the National Research Foundation (NRF) funded by the Ministry of Science, ICT & Future Planning under contract No. NRF-2016 M1A5A1027456; the project of the Ministry of Ocean and Fisheries under contract No. PG51010.

*Corresponding author, E-mail: baeksh@kiost.ac.kr

(Chung et al., 1989; Moon et al., 1998; Kwak et al., 2013). The community structures and abundances of plankton, the main source of primary production, are closely associated with fish catch fluctuations (Zhang et al., 2000; Kang et al., 2002). The complex physical and chemical characteristics of this area caused by the combination of the warm and cold currents have a significant effect on the population structures and quantitative changes of plankton. Specifically, nutrients are a major factor in regulating the primary production. The spring phytoplankton bloom is generally caused by nutrient dynamics resulting from fluctuations and stratification of the sea temperatures. Another major source of nutrients is upwelling. The upwelling process is induced by strong southerly winds in the southern coastal area of Korea, and plentiful nutrients are transported to the Ulleung Basin along the EKWC. One of the main reasons for the high primary production is the supply of nutrients from upwelling (Hyun et al., 2009; Yoo and Park, 2009) and eddies (Kim et al., 2007a); however, there have been no studies on the direct biological responses to the availability of nutrients in this area.

In addition to upwelling, wind can generate episodic events that affect primary productivity in the marine ecosystem. Episodic windstorm events, resulting from the passage of low-pressure systems over ocean areas, can significantly change aquatic ecosystems with their powerful winds (Ryan et al., 2002; Zhao et al., 2008; Tsuchiya et al., 2014). The wind-induced "island effect" can occur near islands (Gilmartin and Revelante, 1974; Hernández-León, 1991). The Ulleung Basin has only two islands: Ulleungdo and Dokdo. Baek et al. (2018) recently reported that the episodic windstorm events in spring play an important role in triggering large phytoplankton blooms in oligotrophic waters in the vicinity of Dokdo. Furthermore, the generation and extinction times of phytoplankton blooms are related to wind speed and duration. Strong winds from a typhoon could delay the timing of spring blooms in the East Sea (Kim et al., 2007b), and they can accelerate the extinction of blooms by scattering the phytoplankton. The southerly wind effects on the upwelling phenomenon have been well studied; however, the effects of episodic strong winds from all directions have been rarely reported in the Ulleung Basin of the East Sea.

The populations of phytoplankton, which drive primary production, are constantly flowing into the East Sea, including the Ulleung Basin, through the EKWC, which branches from the Tsushima Warm Current (Kim et al., 2018; Park et al., 2018), and the eutrophic southern coastal area of Korea also has an important function to supply an abundance of phytoplankton to the Ulleung Basin (Lee et al., 1998; Kang et al., 2005; Oh et al., 2004). To understand the origin and fluctuation of primary production in the East Sea, a tracking survey of the phytoplankton population is needed; however, research on the currents taken by phytoplankton have been rare.

Many individual phytoplankton studies (Kim et al., 2007b; Kim et al., 2012; Tsuchiya et al., 2014) and chlorophyll analyses using satellites (Mooers et al., 2005; Liu and Chai, 2009; Yoo and Park, 2009) have been performed to explain the high primary production in the East Sea; however, an ocean physical, chemical, and biological survey must be performed to understand primary production in this complex marine ecosystem. The present study provides horizontal and vertical analyses of the physical, chemical, and biological features along the EKWC from the southern coastal area of Korea to the Ulleung Basin based on data collected in spring 2017. In addition, bioassay was performed to estimate the variation in the primary production caused by the introduction of nutrients using natural seawaters in spring.

2 Materals and methods

2.1 *Sampling stations and dates*

The survey was conducted from May 27 to 30, 2017 (spring); 29 stations around the Ulleung Basin (from the southern coast of Korea to Dokdo) in the East Sea were surveyed to understand the oceanographic characteristics that affect primary production in spring (Fig. 1). The sampling route was determined by referring to the average path (in May) of the Tsushima Warm Current over the past 20 years, which was based on date from the Korea Meteorological Administration (KHOA; http://www.khoa.go.kr) (Fig. 1a). For effective data analysis, the 29 stations were divided into three areas based on oceanic and geographical features. The coastal area of Korea where upwelling occurs frequently, including the Nakdong River Estuary, is referred to as CS area (Coastal Stations: 1–6). The offshore open area that contains the Ulleung Basin is referred to as OS area (Offshore Stations: 7–9 and 12–15). The wa-

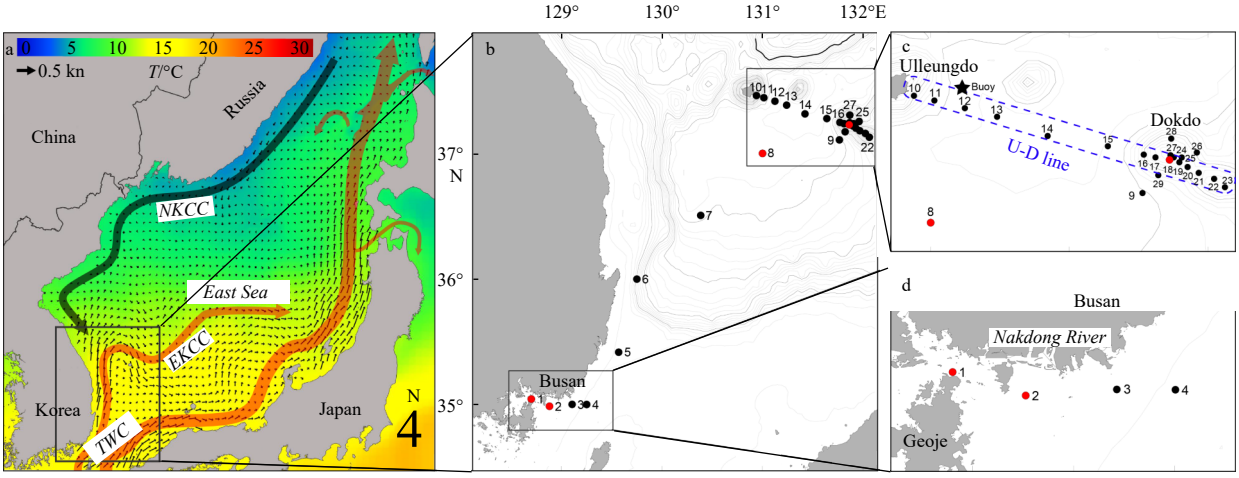

Fig. 1. Average satellite-derived surface current and sea surface temperature (T) for 20 years in May (a) and the locations of sampling stations (b, c, d). The red circles indicate the stations for the bioassays. The star mark shows the location of the Ulleungdo Ocean Data Buoy (Korea Meteorological Administration). The background contours represent isobaths.

ter in the vicinity of Ulleungdo and Dokdo, which can be affected by the "island effect", is referred to as IS area (Island Stations: 10 and 11 in the vicinity of Ulleungdo and 15–29 in the vicinity of Dokdo) (Figs 1b–d).

2.2 *Wind and satellite data*

Time series data for air pressure, maximum wave height, wind gust speed and wind direction were obtained from the Ullengdo Ocean Data Buoy (Korea Meteorological Administration), which takes measurements at 1-h intervals (Fig. 1c); the data spanned May 15 to 31. Satellite-derived geostrophic surface current and sea surface temperature data obtained from Korea Ocean Satellite Center.

2.3 *Horizontal survey*

The horizontal survey was performed using the R/V *Eardo* for all 29 stations. Water temperature, salinity, pH, and dissolved oxygen of surface water (depth of 0.5 m) were measured at each station using a YSI meter (YSI 6600 data sonde, USA). Water samples for nutrient analysis were filtered (GF/F; 25 mm, pore size 0.45 μm; Whatman, Middlesex, UK), placed in acid-cleaned polyethylene bottles, and fixed using $HgCl_2$ (Parsons, 2013). Each filtered water sample was stored at –20°C for future analysis. The ammonium, nitrate, nitrite, phosphate, and silicate concentrations were determined in the laboratory using a flow injection autoanalyzer (Quattro 39; Seal Analytical, Fareham, Hampshire, United Kingdom). The nutrient concentrations were calibrated using Reference Materials for Nutrients in Seawater (RMNS, KANSO Technos Co., Ltd., Japan). For chlorophyll *a* (Chl *a*) measurements, 0.5 L of each water sample was filtered through a 47-mm diameter glass fiber filters (pore size 0.7 μm, Whatman, Middlesex, UK), and the filter was stored at –20°C until further laboratory analysis. Moreover, Chl *a* was measured using a Turner Design fluorometer (10-AU; Turner BioSystems, Sunnyvale, CA, USA) following the extraction of the filtered material with 90% acetone in the dark for 24 h. Furthermore, 0.5-L subsamples were stored in polyethylene bottles to identify and enumerate phytoplankton and fixed with 0.5% Lugol's solution. These subsamples were then concentrated to approximately 50 mL by decanting the supernatant, as described by Sournia (1978). A Sedgewick-Rafter counting chamber was used to estimate the abundance of phytoplankton using light microscopy, and phytoplankton cells were identified at the species level. Differences in measurements among the abiotic and biotic factors in the CS, OS and IS areas were assessed using an analysis of variance (ANOVA) followed by a Tukey's test. All statistical analyses were performed using SPSS version 17.0 (SPSS, Inc., Chicago, IL, USA).

2.4 *Vertical survey*

The vertical survey was conducted from the sea surface to the sea bottom at 14 stations located between Ulleungdo and Dokdo (U-D line) to understand the characteristics of the water masses in the study area (Fig. 1c). The vertical profiles of temperature, salinity, water density (sigma-*t*), and fluorescence were measured using a conductivity, temperature, and depth (CTD) sensor (SBE 911 plus CTD; SeaBird Inc., Bellevue, WA, USA) mounted on a rosette sampler of the R/V *Eardo*. Additionally, water samples from five selected stations (Stas 10, 12, 13, 18, and 22) were collected from the surface to a depth of 200 m using a rosette sampler to measure Chl *a* and nutrient concentrations, which were estimated using the same methods, as described above.

2.5 *Nutrient addition bioassays*

The bioassays were designed to assess the biological reaction of phytoplankton to the introduction of nutrients in the Ulleung Basin. First, the biological activity of the phytoplankton at all stations, including *in vivo* Chl *a*, active Chl *a*, and biological activity (F_v/F_m), were measured using a Phyto-PAM instrument (phytoplankton analyzer; PHYTO-ED, Germany) to determine the bioassay stations; four stations (two stations in the CS area and one each in the OS and IS areas) were selected according to the Chl *a* and biological activity measurements. To avoid contamination of experimental container, all polycarbonate bottle and instruments used in the experiment were previously soaked in 10% hydrochloric acid and rinsed with deionized water (Milli-Q system, Millipore) before use. Then, 200-mL subsamples collected at the four stations were transferred to acid-washed polycarbonate culture flasks (JetBiofil® Treated Culture Flasks, Sterile, 250 mL) and immediately incubated in an acrylic culture water bath (Fig. 2), which was designed to culture organisms under conditions of natural field light and seawater temperature, for two weeks aboard the R/V *Eardo* and then at the pier after the vessel's cruise. Incubations were carried out in acrylic boxes continuously cooled with surface water. A pump was used to circulate sea water around the acrylic culture bath. To exclude an excessive feeding effect of zooplankton, a 330-μm sieve was used to remove zooplankton and debris from the water samples. The control used seawater without added nutrients. The treatments included the addition of (1) nitrogen (+N; 20 μmol/L nitrate), (2) phosphorus (+P; 2 μmol/L phosphate), and (3) nitrogen and phosphorus (+NP; added at the same concentrations as for the +N and +P treatments alone). Silicates (20 μmol/L silicate) were added to all the experimental groups including the controls. The growth responses of each flask were measured by the concentration of *in vivo* Chl *a* using the Phyto-PAM instrument at one- or two-day intervals for 12 or 14 d. Based on the assumption that *in vivo* Chl *a* is a quantitative measure of algal biomass, the growth

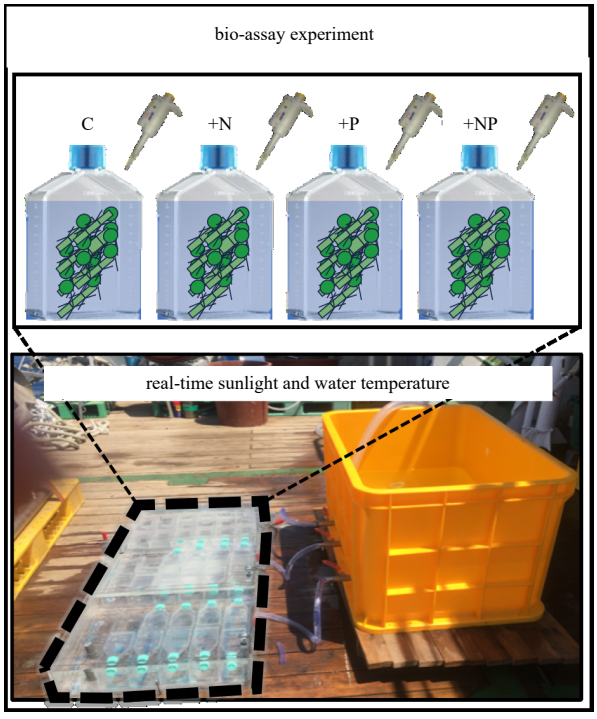

Fig. 2. Illustration of the nutrient addition experiments.

rate (d^{-1}) was calculated by linear regression as the slope coefficient: $\ln(Fl_t) = \mu \times t + \ln(Fl_0)$, where Fl_0 and Fl_t are the *in vivo* Chl *a* at the start of the experiment and after *t* days of incubation, respectively, according to the protocol of Baek et al. (2015). In particular, the algal growth has responded in early stages for Stas 1 and 2 of coastal station. However, growth response was not unfortunately observed in early stages for Stas 8 and 18 of offshore station, due to which was depend on the initial population density and algal community structure in each sampling station. Based on the time-series algal growth curve in each bioassay, specific algal growth response was calculated from beginning to 4 d for Stas 1 and 2, 10 d for Sta. 8, and 8 d for Sta. 18. In addition, the nutrient concentrations of each flask were measured to evaluate the relationship between nutrient disappearance and phytoplankton response. The subsamples (10 or 20 mL) were taken from each flask during the middle of the experiment (on Day 5 for Stas 1 and 2, Day 7 for Sta. 8, and Day 6 for Sta. 18) and the end of the experiment (on Day 12 for Stas 1 and 2, Day 10 for Sta. 8, and Day 9 for Sta. 18). Then, each subsample was immediately filtered using a disposable syringe filter (pore size 0.45 μm; ADVANTEC), fixed with $HgCl_2$, and stored at –20°C. The nutrient analysis was performed following the same methods described above. The bioassay data were analyzed using the *t*-test to compare the results of nutrient treatments and control groups. Differences were considered significant at $p<0.05$.

3 Results

3.1 *Episodic windstorm and current effect*

The time series of air pressure (hPa), maximum wave height (m), wind gust speed, and wind direction measured at the Ulleungdo Ocean Data Buoy are shown in Fig. 3. On May 25, a strong cyclone (998.5 hPa) passed through the Ulleung Basin, and the wind direction shifted from a southwest wind to an extremely strong northwest wind. The highest wave height was 6.3 m, and the wind speed was 18.3 m/s. During the survey period, this low pressure disappeared, and northeast winds shifted back to southwest winds. The surface water temperature (determined by a satellite-derived temperature image) was approximately 10–16°C in the northwestern region and approximately 15–20°C in the southwestern region, with a front marking differences in water temperature at approximately 38°N (Fig. 4).

3.2 *Physicochemical features*

Our field measurements showed that the surface water temperature ranged from 16.4°C to 18.6°C, with an average of (17.4±0.52)°C, and the geographical variation was not large (Fig. 5a); the ANOVA results indicated that the differences were not significant (Fig. 5c). The surface salinity varied from 33.2 to 34.5, with an average of 34.2±0.31. Specifically, for the CS area located near land, i.e., where the discharge of fresh water into coastal waters

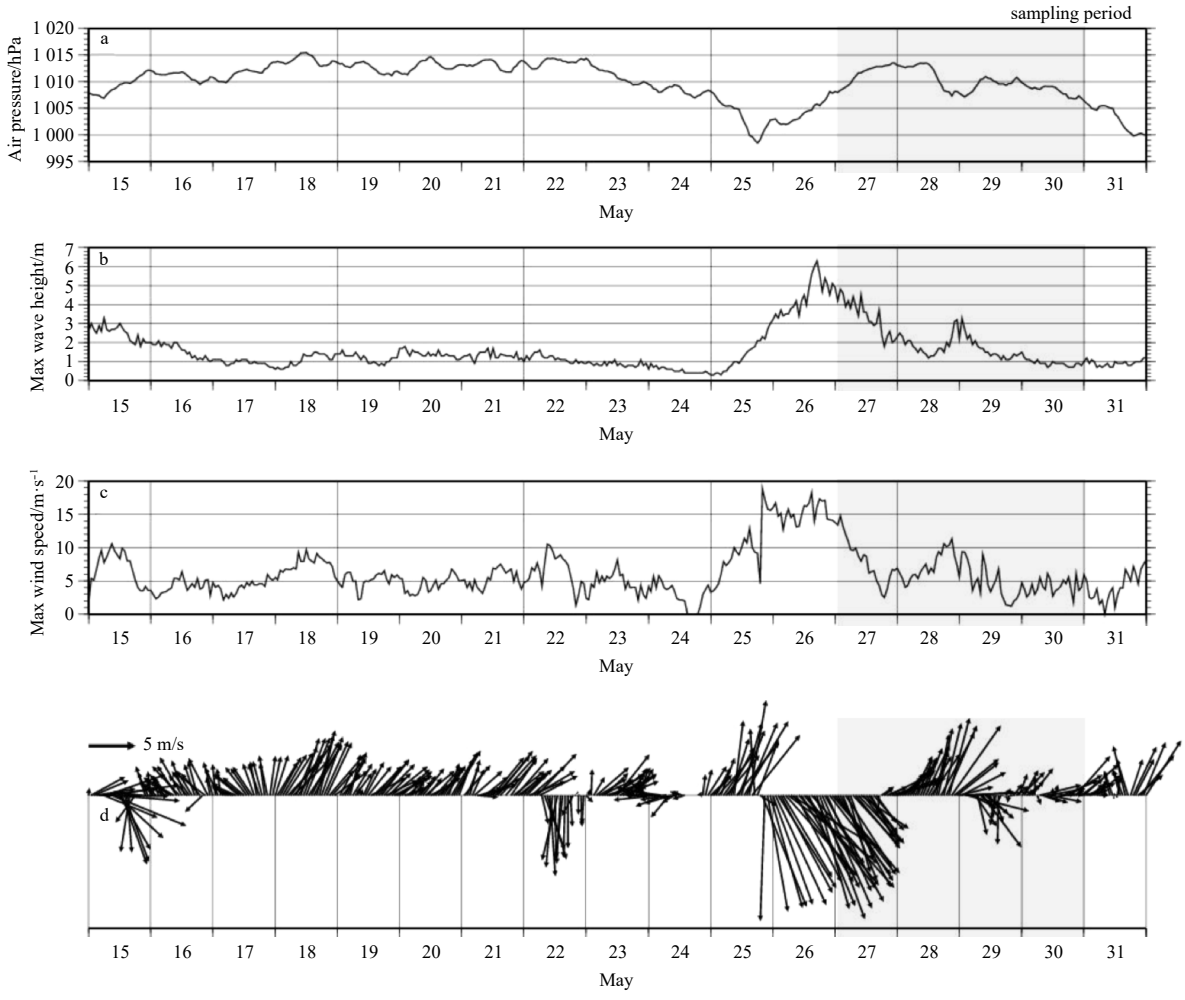

Fig. 3. Time series of air pressure (hPa) (a), maximum wave height (m) (b), wind gust speed (m/s) (c), and wind direction (d) from 15 to 31 May 2017 at the Ulleungdo Ocean Data Buoy (Korea Meteorological Administration).

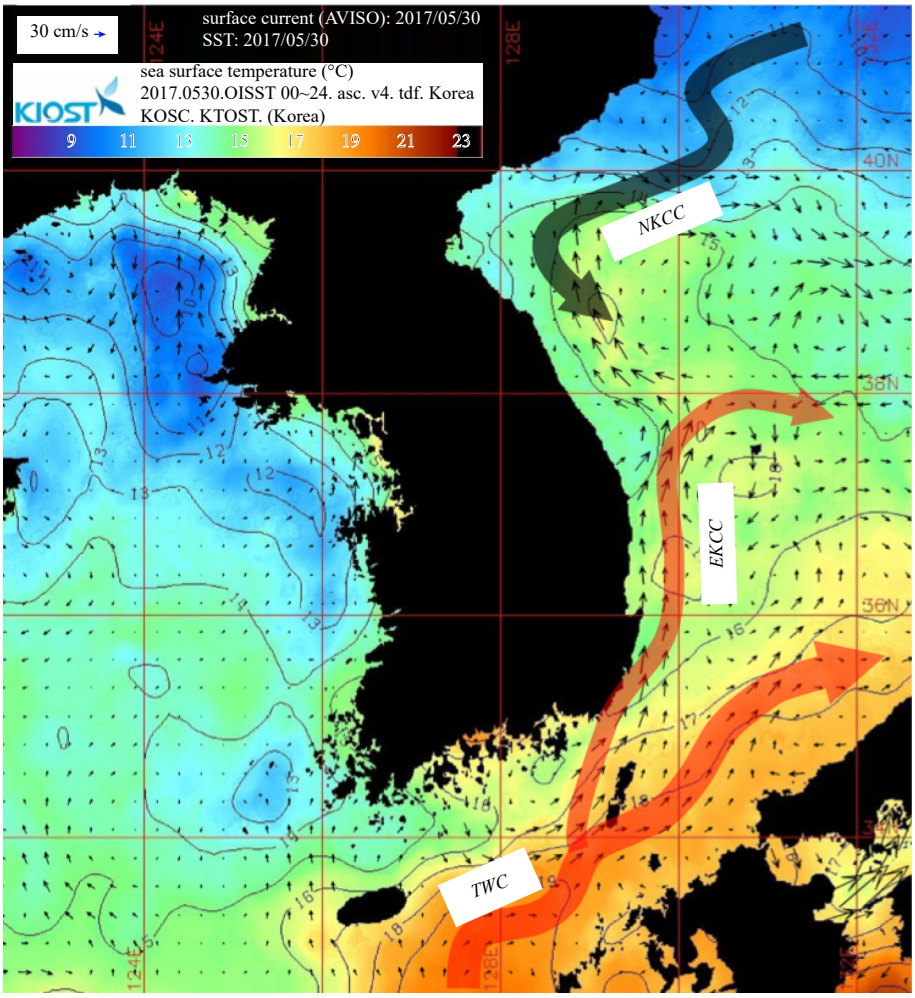

Fig. 4. Satellite-derived geostrophic surface current and sea surface temperature for May 30, 2017.

occurs, the average salinity was 33.7±0.28, which was significantly lower than at the OS and IS areas (F=40.99, p<0.001) (Figs 5a, d). Dissolved oxygen at the CS area ranged from 7.66 to 8.68 mg/L, with an average of (8.21±0.36) mg/L, and the mean dissolved oxygen at the OS and IS areas was (7.97±0.08) mg/L (Fig. 5b). The dissolved oxygen values at the CS area were significantly different than those of the OS and IS areas (F=7.757, p<0.01) (Fig. 5e). The pH value varied from 8.04 to 8.26, with an average of 8.19±0.04. Notably, the pH at Sta. 1 was slightly lower (Fig. 5b), and the pH values measured at the CS area were significantly different from only the IS area (F=4.700, p<0.05) (Fig. 5f). Dissolved inorganic nutrients displayed large spatial variations (Fig. 6). Among the CS area, the nutrient concentrations at Stas 1 and 2 were higher than those of the other stations: the nitrate+nitrite values were 4.92 and 3.09 μmol/L (Fig. 6a), the ammonium values were 2.04 and 0.41 μmol/L (Fig. 6b), the phosphate values were 0.38 and 0.20 μmol/L (Fig. 6c), and the silicate values were 9.98 and 7.87 μmol/L (Fig. 6d), respectively. From Stas 3 to 29, nitrate+nitrite varied from 0.87 to 1.73 μmol/L, with an average of (1.31±0.20) μmol/L; ammonium varied from 0.01 to 1.03 μmol/L, with an average of (0.23±0.23) μmol/L; and phosphate and silicate had average values of (0.06±0.02) μmol/L and (3.89±0.50) μmol/L, respectively. Consequently, the nutrient concentrations at the CS area were significantly different from the OS and IS areas (Figs 6e–h). Except for temperature and pH, all of physicochemical features of the CS area were distinguishable from the OS and IS areas (nitrate+nitrite: F=4.599, p<0.05; silicate: F=6.419, p<0.01; ammonium: F=1.481, p>0.05; and phosphate: F=2.156, p>0.05); however, there were no differences between the OS and IS areas according to the ANOVA results.

3.3 *Characteristics of Chl a and phytoplankton*

The concentration of surface Chl *a* at each station varied from 0.07 to 2.34 μg/L, with an average of (0.33±0.53) μg/L. The concentrations at the CS area were significantly higher than the other areas (F=10.74, p<0.001), and the abundances of phytoplankton exhibited similar fluctuations with Chl *a* (Fig. 7a). The abundances of phytoplankton at each station varied from 0.20×10^5 to 4.15×10^5 cell/L, with an average of (1.91±1.66)×10^5 cell/L at the CS area. Higher phytoplankton abundances at Stas 1 and 3 were estimated to be 4.15×10^5 and 3.83×10^5 cell/L, respectively. The relative ratio of phytoplankton at the CS area included 75.1% Bacillariophyceae, 11.1% Dinophyceae, and 7.26% Cryptophyceae (Fig. 7b). Specifically, the diatoms *Leptocylindrus danicus* (26.6%) and *Chaetoceros* spp. (25.1%) appeared as the dominant species (Fig. 7c). The abundances of phytoplankton at the OS and IS areas varied from 0.02×10^4 cell/L to 0.12×10^4 cell/L, with an average of (0.06±0.03)×10^4 cell/L; of these, Bacillariophyceae comprised 40.0% and 43.6% of the community. Bacillariophyceae were mainly present as *Rhizosolenia setigera*, and other

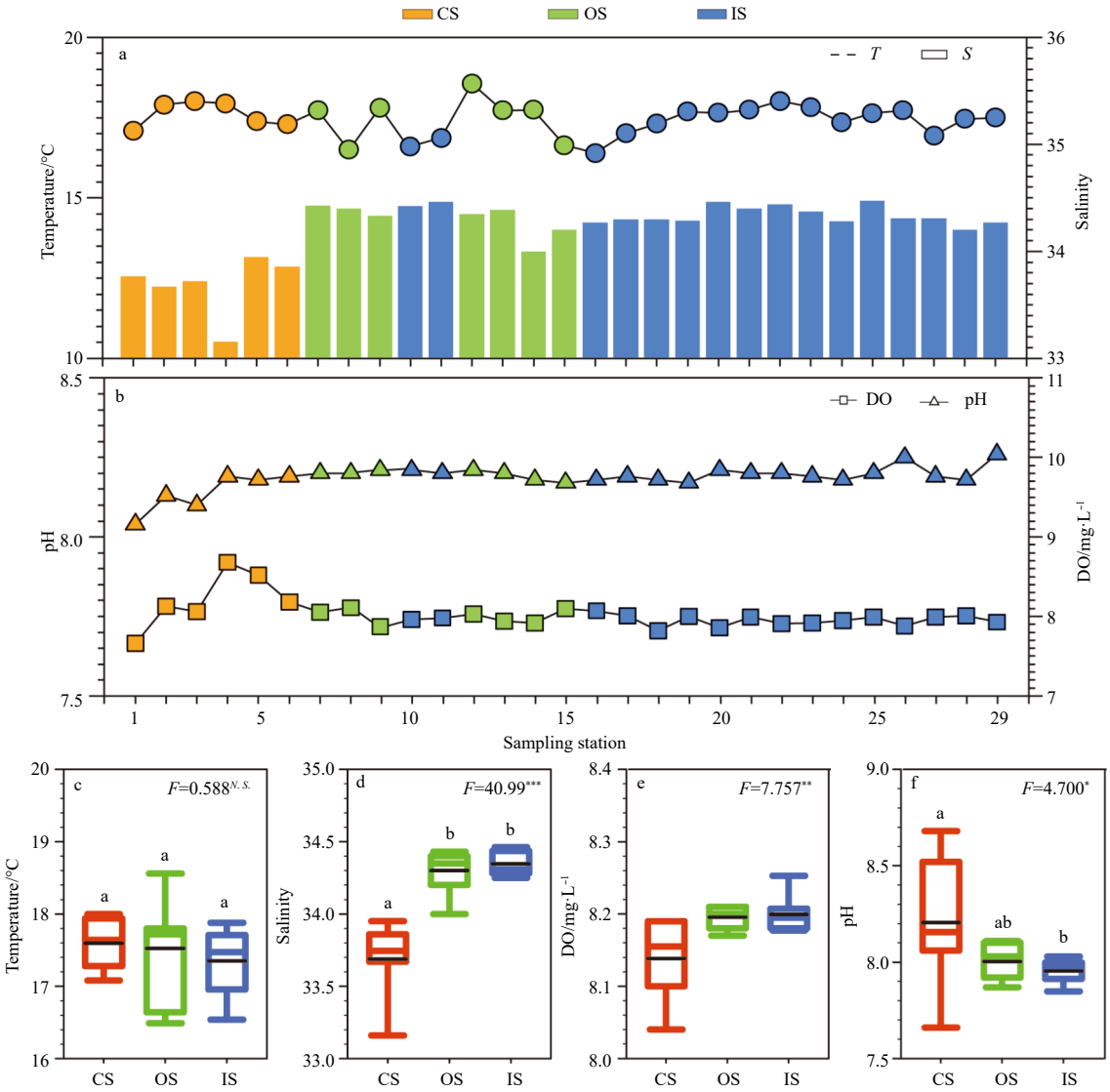

Fig. 5. Horizontal distribution of temperature and salinity (a) and pH and DO (b) at the sampling stations in the East Sea. Comparison of abiotic factors (c–f) in three designated zones in the study area in the East Sea. The data are presented as the mean±standard errors of the sampling data for each zone. The results were analyzed using one-way ANOVA and Tukey's post hoc test. Letters a and b represent significant differences (p<0.05), *N.S.* not significant, *** p<0.001, ** p<0.01, and * p<0.05.

species included unidentified nano-flagellates.

3.4 *Vertical characteristics of water mass along the U-D line*

The vertical profiles of water temperature, salinity, density, and fluorescence along the U-D line are shown in Fig. 8. The vertical extent of relatively high temperatures (ca. 17°C) following the origin of the TWC remained within the top 50 m. However, in the central area (from Stas 14 to 16), this warm water only extended to a depth of 30 m (Fig. 8a). In addition, the mixed water mass with temperatures ranging from 5 to 13°C extended to a depth of 200 m near Ulleungdo, whereas it remained at a depth of approximately 100 m in the central area of the U-D line; the mixed water mass deepened gradually to a depth of 130 m near Dokdo (Fig. 8a). The characteristics of the vertical distribution of salinity were similar to those of the temperature (Fig. 8b). A relatively high saline (34.5) water mass deepened gradually in the waters around Ulleungdo, and the 34.2 isohaline persisted to a depth of 150–170 m; for higher depths, the salinity remained below 34. The vertical pattern of the water density (sigma-t) was arranged with a vertical water temperature pattern ranging from 24.0 to 27.2 kg/m^3 (Fig. 8c). From the vertical fluorescence values, the subsurface chlorophyll maximum (SCM) was found between depths of 30 and 50 m along the U-D line; however, the SCM layer was not well defined around Ulleungdo and Dokdo because it spread toward the surface layer (Fig. 8d).

Vertical fluorescence values and nutrient concentrations of five selected stations along the U-D line are shown in Fig. 9. Except for Sta. 10, the SCM layer along the U-D line appeared at depths of 30–50 m (Figs 9a–e). The concentrations of nitrate+nitrite (Figs 9f–j), phosphate (Figs 9p–t), and silicate (Figs 9u–y) remained low in the surface layer (approximately 50 m), although their concentrations increased gradually below 50 m. Ammonium was generally high in the surface layer and very low at depths below 50 m (Figs 9k–o). Specifically, the lowest ammonium concentration in the surface layer was observed at Sta. 11 where chlorophyll *a* was high in the surface layer, and it was also high at

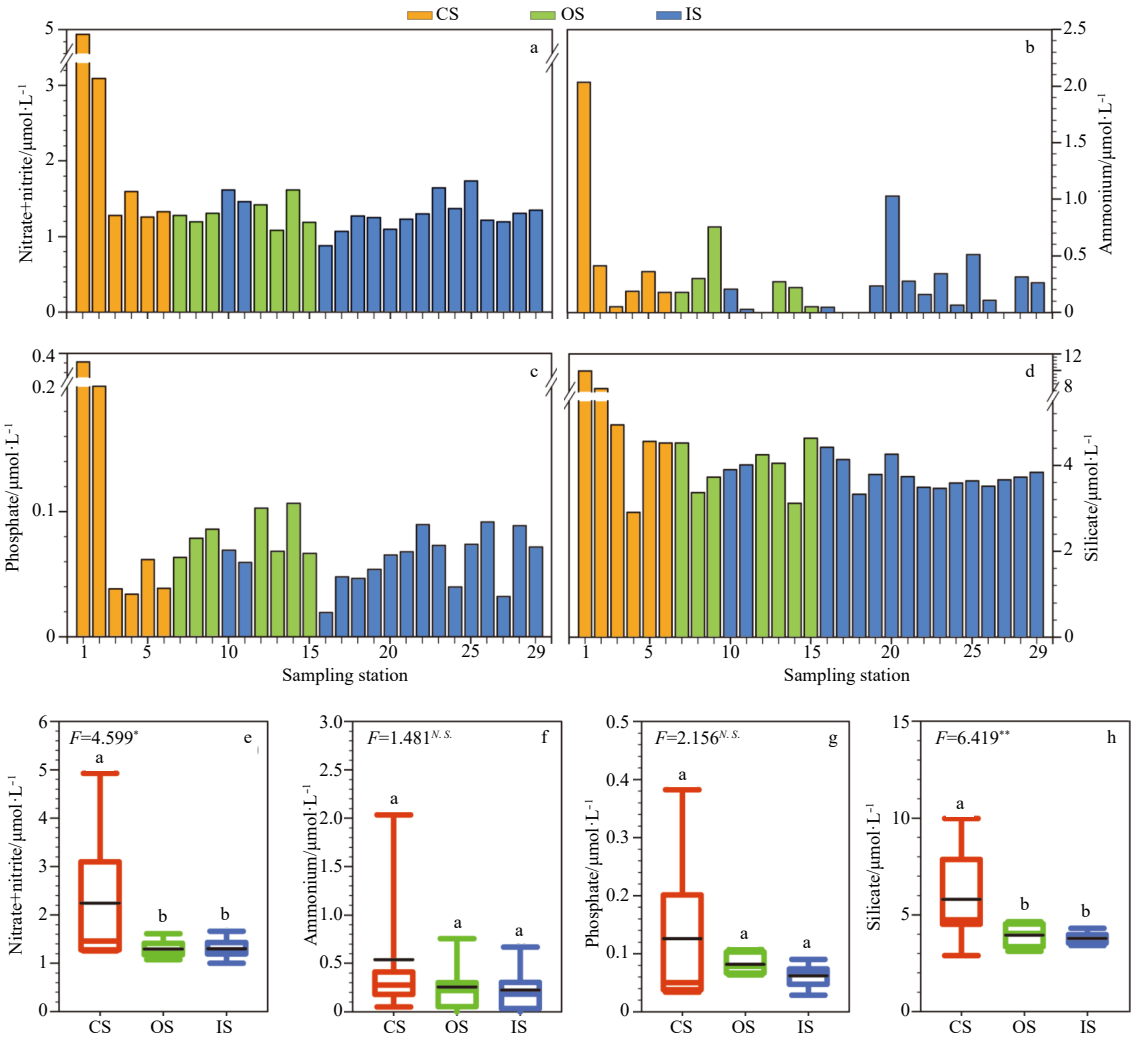

Fig. 6. Horizontal distribution (a-d) of nutrients at the sampling stations and comparison of nutrients (e–h) in three designated zones in the study area in the East Sea. a. nitrate+nitrite, b. ammonium, c. phosphate, and d. silicate. The data are presented as the mean±standard errors of the sampling data for each zone. The results were analyzed using one-way ANOVA and Tukey's post hoc test. Letters a and b represent significant differences (p<0.05), *N.S.* not significant, *** p<0.001, ** p<0.01, and * p<0.05.

the bottom of Sta. 19. The N:P ratio in the upper layers of the SCM exceeded 16, and the ratio decreased gradually as the water depth deepened (Figs 9z–d').

3.5 *Growth responses of phytoplankton to nutrients*

The values of *in vivo* Chl *a* based on the Phyto-PAM for each station were measured to select the seawater samples for bioassay; the concentrations ranged from 0.01 to 3.00 μg/L (Fig. 10a). The *in vivo* Chl *a* was relatively high at the CS area. Specifically, the values at Stas 1 and 2 were 2.01 μg/L and 3.00 μg/L, respectively. At the OS and IS areas, the values of Chl *a* were consistently very low, averaging (0.29±0.32) μg/L. The concentration of active Chl *a* was approximately 1/3 of the concentration of *in vivo* Chl *a*, as shown by Phyto-PAM, and the tendency was the same. Regarding biological factors, Chl *a*, *in vivo* Chl *a*, active Chl *a*, and F_v/F_m based on Phyto-PAM at the CS area were significantly higher than those at the OS and IS areas (Chl *a*_PAM: F=11.36, p<0.001; active Chl *a*: F=11.18, p<0.001; ANOVA) (Figs 10b–e). The experiment was designed with concentration gradients in Chl *a*. The target concentrations of Chl *a* were high than 2, (0.5±0.05), and (0.1±0.01) μg/L, although the seawater samples of biological activity (F_v/F_m) less than 0.1 were excluded from the test. Consequently, the seawater samples from Stas 1 and 2 in the CS area, those of Sta. 8 for 0.5 μg/L of Chl *a*, and those of Sta.18 for 0.1 μg/L of Chl *a* were selected.

The temporal variation in the bioassay growth of phytoplankton cultured in the control and the +N, +P, and +NP treatments is shown in Fig. 11. The growth responses of phytoplankton were higher in the treatments at Stas 1 and 2 than the other treatments at Stas 8 and 18 (Figs 11a–d). The growth rate at Sta. 1 was 0.43 d^{-1} for the control, 0.99 d^{-1} for the +N treatments, 0.67 d^{-1} for the +P treatments, and 1.28 d^{-1} for the +NP treatments (Fig. 11e). The growth rate at Sta. 2 was 0.54 d^{-1} for the control and 1.20 d^{-1} for the +NP treatments (Fig. 11f). The growth rate at Sta. 8 was 0.19 d^{-1} for the control and 0.53 d^{-1} for the +NP treatments (Fig. 11g). At Sta. 18, the phytoplankton growth rate was relatively low in all the treatments including the control (Fig. 11h). In all experiments, the growth responses of the experimental groups of +N and +NP were significantly higher than the other treatments and control groups.

The nutrient consumption trends at the initiation, middle, and final phases of the bioassays are shown in Fig. 12. The initial

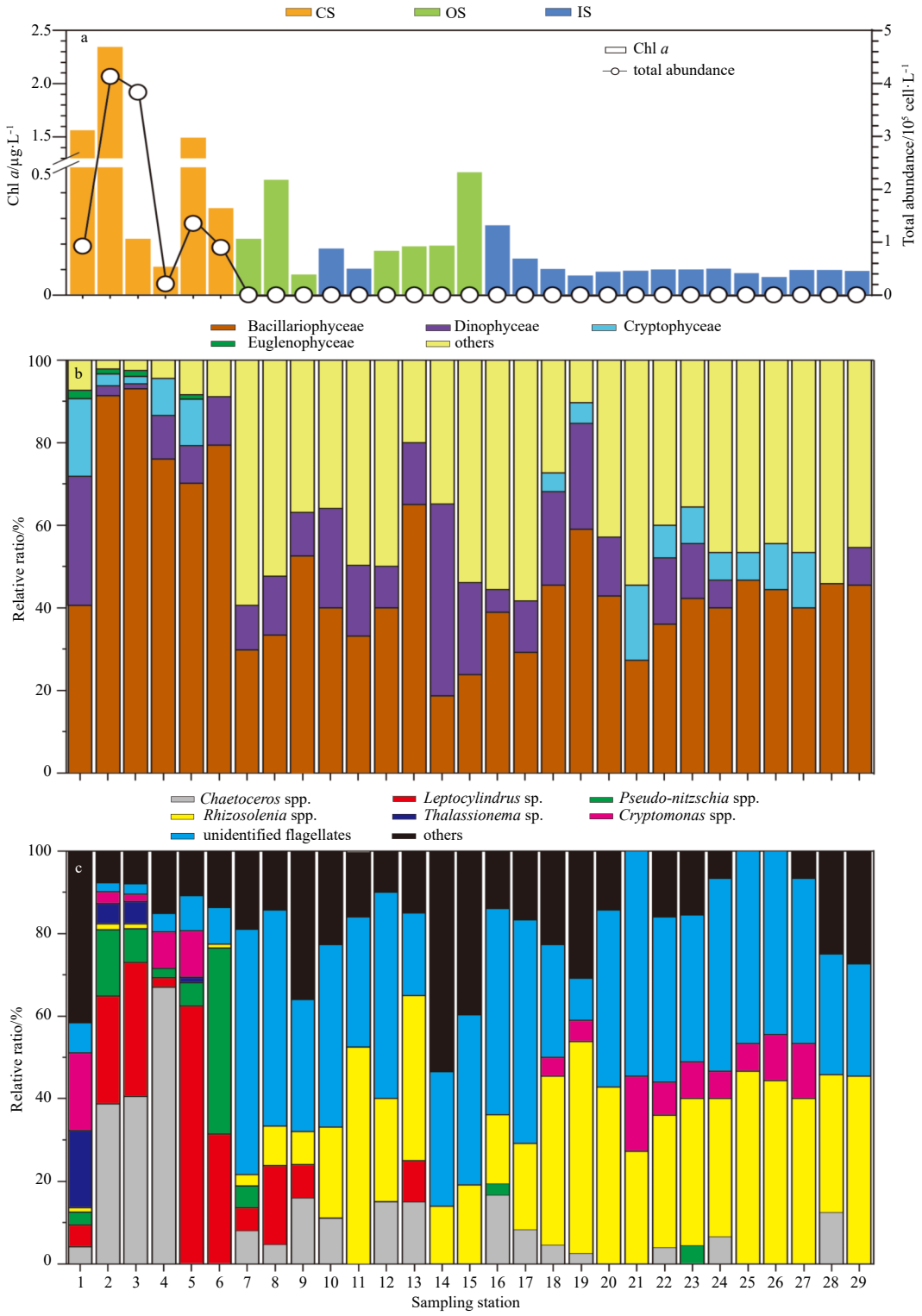

Fig. 7. Horizontal changes in Chl *a* and total phytoplankton abundance (a), relative dominant phytoplankton at the class level (b), and relative dominant phytoplankton at the genus level (c) at the sampling stations in the East Sea.

concentrations of nutrients at the CS area were significantly different from the OS and IS areas (Figs 6e–h); however, the effects on the bioassay may have been small because of sufficient nutrient addition (Figs 12a–d). The phytoplankton in the +N and +NP treatments grew rapidly, and thus, the nitrate+nitrite and the phosphate were depleted from the middle to final phase. Moreover, the rate of nutrient consumption in the +NP treatments was distinctly faster than in the +N treatments (Figs 12e–h and 12m–p). In contrast, the growth responses of all +P treatments were not much higher than the control treatments (Fig. 11). Therefore, the initial nutrients (nitrate + nitrite, phosphate, and silicate) remained (Figs 12i–l). The silicate levels were also con-

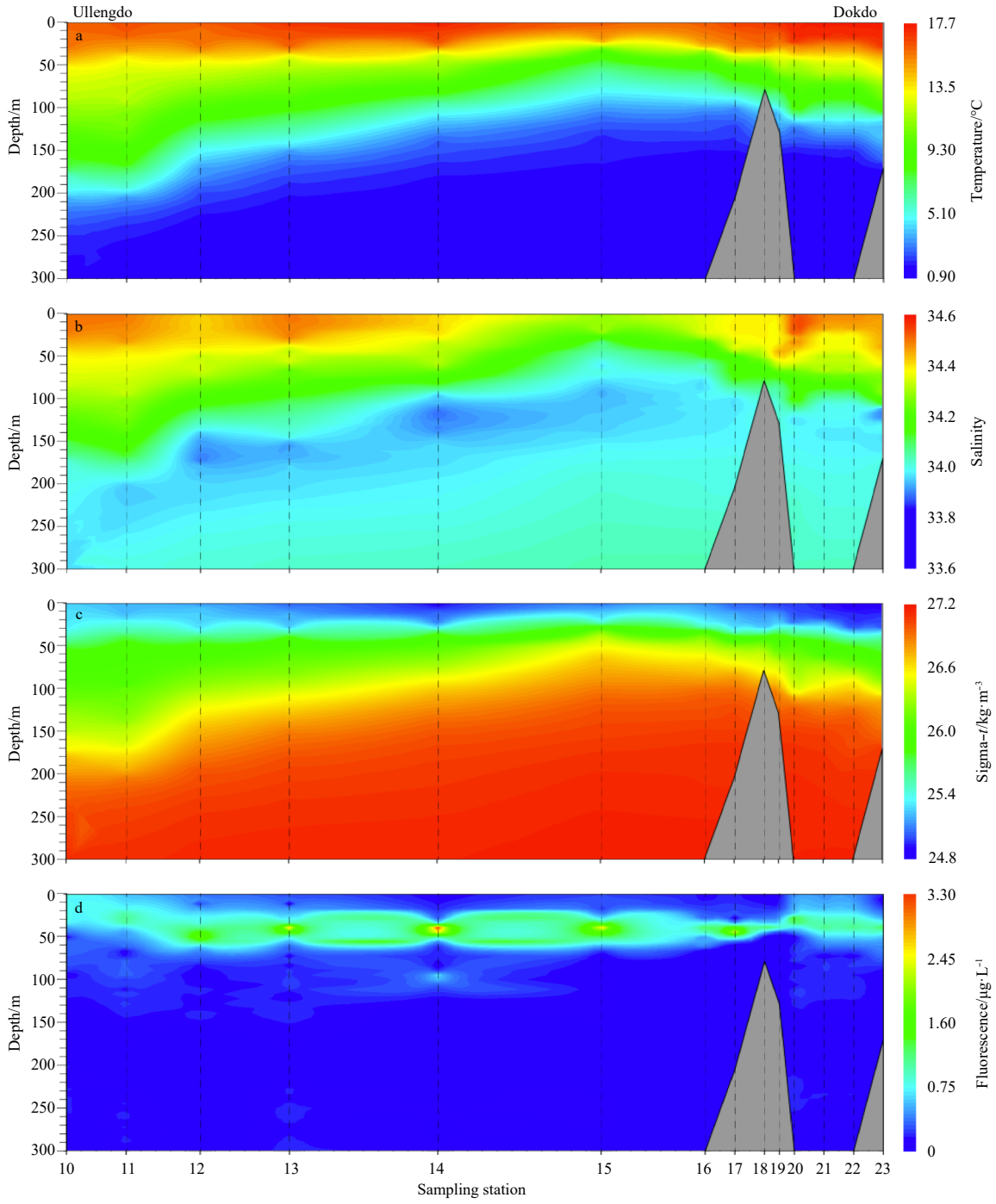

Fig. 8. Vertical distribution of temperature (a), salinity (b), sigma-*t* (c), and fluorescence (d) along the U-D line in the East Sea.

sumed in the +N and +NP treatments; however, the consumption was low in the treatments at Stas 8 and 18 compared with Stas 1 and 2 (Figs 12h and p).

4 Discussion

4.1 *Effects of currents and winds*

Gong and Son (1982) and Mooers et al. (2005) reported that the Ulleung Basin (Ulleungdo-Dokdo line) water mass, located at approximately 38°N, was greatly influenced by the northward flowing East Korea Warm Current (EKWC) and the southward flowing North Korea Cold Current (NKCC), which are interconnected with the oligotrophic warm water origin of the Tsushima Warm Current (TWC) and mesotrophic cold water, respectively; these results demonstrated that there was high primary production in the area where the currents merged. We confirmed the warm eddy area between 36°N and 38°N based on satellite-derived surface temperature and water current data (Figs 1a and 4). In our sampling period, the relatively warm water ranging from 14 to 17°C had greatly extended toward the north into the latitudinal area of 38°–40°N, resulting in the thermal front between the EKWC and NKCC near ca. 40°N (Fig. 4). According to the satellite data of the KHOA, the front was formed at a higher latitude than in other years (data not shown). The effects of this “oligotrophic”

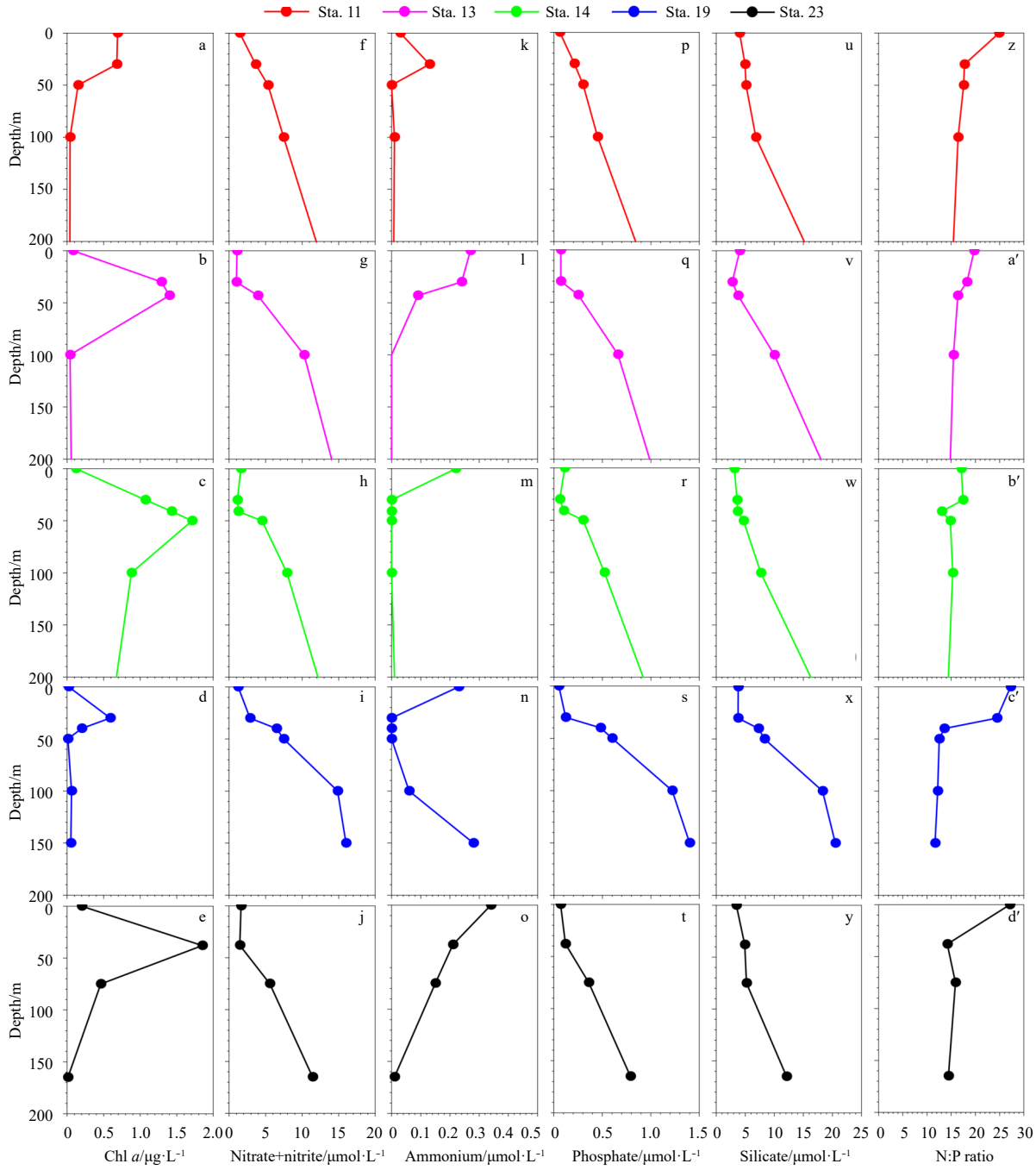

Fig. 9. Vertical changes in Chl *a* (a–e), nitrate+nitrite (f–j), ammonium (k–o), phosphate (p–t), silicate (u–y), and N:P ratio (z–d′) at five selected stations along the U-D line.

warm current must have been stronger than those of other years; thus, low nutrient levels at euphotic layers were widely maintained in the spring of 2017.

In many previous studies, high primary productivity in spring has been identified following the strong southern wind because of the upwelling phenomenon in the southwest region of the East Sea. According to a long-term report by Liu and Chai (2009), phytoplankton biomass in the East Sea increased from the southern area to the central area between March and April before spreading northward in May. Kim et al. (2007b) also demonstrated that spring phytoplankton blooms in the East Sea frequently occurred after a windstorm event but after a time lag; this time lag is when cells accumulate as a result of the water current and phytoplankton growth occurs after nutrient concentrations increase due to water mixing (i.e., upwelling). From our wind results, the relatively weak southwest wind, i.e., <5 m/s, observed from May 15 to 25, shifted to an extremely strong northwest wind (maximum wind speed of 18.5 m/s) due to a low-pressure system (998.5 hPa) that passed through the region on May 25. This shift occurred over 1–2 d before our investigation began. Average wind speed, maximum wind speed, and wind direction in the vicinity of the Ulleung Basin in May for ten years (2006–2015) were collected from the KHOA (Table S1). The windstorm of this survey is an abnormal case compared to the data of the last decade.

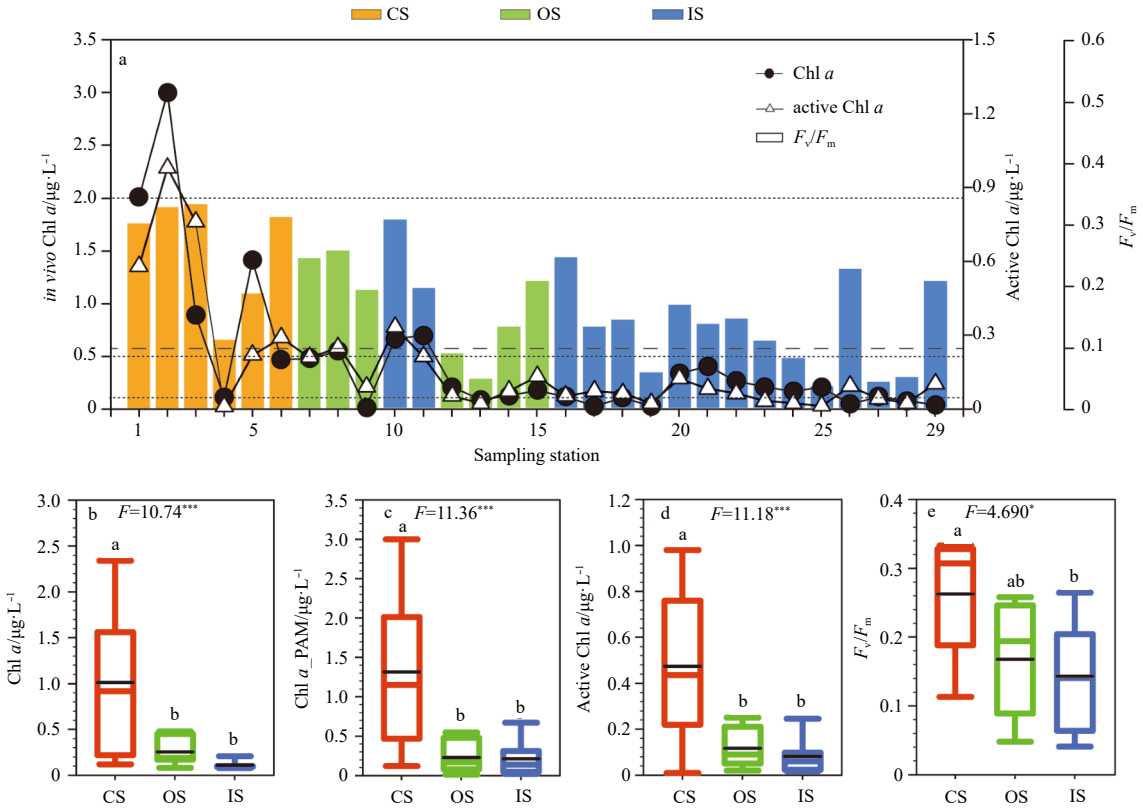

Fig. 10. Horizontal changes in *in vivo* Chl *a*, active Chl *a*, and F_v/F_m based on Phyto-PAM measurements at the surface sampling stations in the East Sea; and comparison of biotic factors (b–e) in three designated zones in the study area in the East Sea. The data are presented as the mean±standard errors of the sampling data for each zone. The results were analyzed using one-way ANOVA and Tukey's post hoc test. Letters a and b represent significant differences (p<0.05), *N.S.* not significant, *** p<0.001, ** p<0.01, and * p<0.05.

The weak southwest wind and strong northwest wind might have suppressed upwelling. As a result, sufficient nutrients were not supplied (Fig. 7), and Chl *a* and phytoplankton biomass remained consistently low in the upper layer of the euphotic zone around the Ulleung Basin (Fig. 7). In contrast, when a similar cyclone (998.3 hPa; maximum wind of 27.6 m/s) dominated by southwest winds passed through the study region 1–2 d before sampling began in May 2016, large phytoplankton blooms occurred in the water around Ulleungdo and Dokdo (Baek et al., 2018).

Additional satellite data obtained from Korea Ocean Satellite Center showed high Chl *a* concentrations (around >5 mg/m^3) in the northwestern region of the East Sea on May 19, 2017 (Fig. S1a); however, this area may have been greatly diluted or spread out by the strong northwest wind that began on May 25 (Fig. 3). Thus, Chl *a* remained low in the central East Sea, including the Ulleungdo and Dokdo areas, through May 27 (Fig. S1b; our sampling period) and June 3 (Fig. S1c; after a week). All of the results imply that the currents and both wind speed and direction play important roles in regulating the dynamics of phytoplankton blooms and primary production in the southwest region of the East Sea.

4.2 *Oceanographical interactions between coastal and offshore regions of the East Sea*

It is generally believed that coastal and estuarine waters have nutrient-rich conditions, and the nutrient concentrations of inshore waters decrease gradually toward the continental shelf of offshore waters, resulting in poor nutritional status in open areas (Smith et al., 1999; Wasmund et al., 2001; Zhang et al., 2007). To compare the features of environmental factors and phytoplankton biomass, to understand the relationship between the coastal and offshore waters, and to consider the "island effect", our survey area was divided into three zones (CS, OS and IS) based on geo-oceanographical features.

Overall, the abundances of phytoplankton and Chl *a* concentrations were relatively low in May 2017 (Fig. 7). What is the driving force to maintain the high productivity of the offshore area of the East Sea? The southeastern coastal area of Korea is known as an area with high primary productivity that experiences frequent upwelling events after strong southerly winds that dominate from spring to summer (Lee, 1983; Lee and Na, 1985; Yoo and Park, 2009). In addition, the water mass with high primary production is transferred by the EKWC, and the high phytoplankton biomass is moved by water currents to meet with the NKCC at 37°–38°N before shifting to the east. As a result, the high phytoplankton biomass in the southeastern coastal area moves toward Ulleungdo and Dokdo, which is located 200–300 km off the coastal mainland area. According to the combination of field surveys and satellite-derived Chl *a* images by Hyun et al. (2009), the enhanced biological production caused by wind-driven coastal upwelling after the dominance of southwest winds in the southeastern area of the Korean Peninsula influences the offshore waters in the vicinity of Ulleungdo and Dokdo. Here, we can suggest several possible explanations for the nutrient availability required to maintain high biological production in the oligotrophic offshore waters near Ulleungdo and Dokdo, including the southeastern coastal waters of the Korean Peninsula. First, the nutrients flowing into the estuaries and coastal water from the Nakdong River,

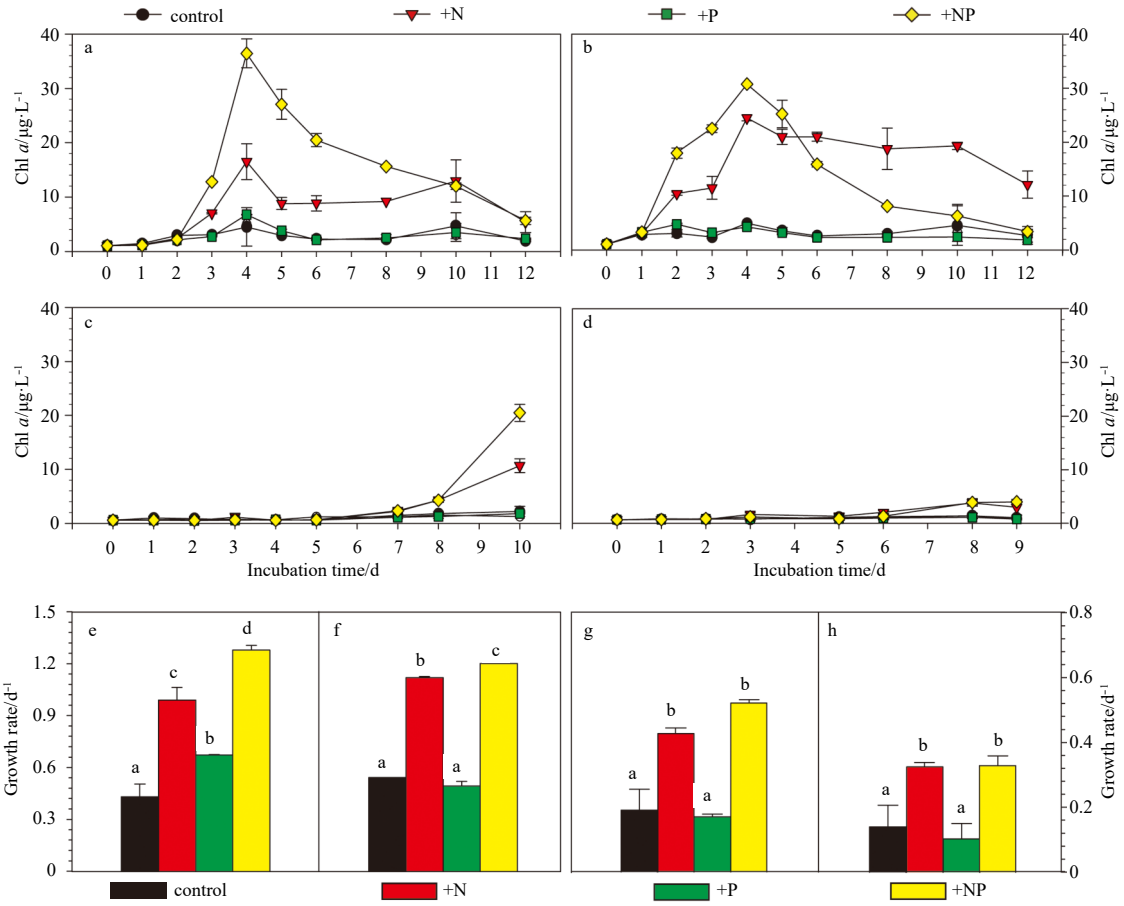

Fig. 11. Change in *in vivo* Chl *a* for phytoplankton assemblages during nutrient addition algal bioassays: Sta. 1 (a), Sta. 2 (b), Sta. 8 (c), and Sta. 18 (d); and specific growth rate of phytoplankton assemblages: Sta. 1 (e), Sta. 2 (f), Sta. 8 (g), and Sta. 18 (h). Control: no nutrient addition; +N: nitrate added; +P: phosphate added; +NP: nitrate and phosphate added. Data are presented as the mean±standard errors for triplicate samples.

the largest river in Korea, in Busan (Fig. 1d), along the eastern coastal area of the Korean Peninsula play important roles in contributing to the phytoplankton blooms, particularly in the rainy seasons, such as spring and summer. Second, the deep nutrient-rich water moves toward the euphotic layer caused by wind-driven coastal upwelling. Finally, high primary production is related to high nutrient concentrations in the euphotic zone caused by upwelling and river discharge; this mass is transferred to the oligotrophic offshore waters of Ulleungdo and Dokdo by water currents (combination of the EKWC and NKCC at 37°–38°N), resulting in the water shifting to the east, i.e., into the oligotrophic open ocean.

Regarding chemical factors, except for ammonium, the concentrations of nutrients at the CS area were significant (Figs 6e–h), however, the water temperature did not differ significantly between the three zones (F=0.588, p>0.05; ANOVA) (Fig. 5c), and the salinity of the CS area was slightly lower than at the OS and IS areas (F=40.99, p<0.001; ANOVA) (Fig. 5d). The comparisons indicated that the Nakdong estuarine area, including the EKWC region, is slightly influenced by rainfall discharges from the land and rivers in this period. Only nutrient levels at a few stations in the CS area, where affected by discharge of the Nakdong River, were higher than at the OS and IS areas, and the biomass of phytoplankton abundances (also Chl *a*) were higher, although the difference was not large (maximum of 415 cells/mL at Sta. 2). In addition, the species composition of phytoplankton at the CS area was different than at the OS and IS areas (Fig. 7). Phytoplankton at the OS and IS areas might not easily grow because of low phytoplankton abundances with nutrient-poor conditions in the oligotrophic offshore waters. All of the results indicated that the offshore region did not receive enough nutrients and phytoplankton biomass to maintain the high primary productivity from the coastal area in this studied spring. The warm currents were strong in May 2017; however, due to a northern windstorm event along the eastern coast of the Korean Peninsula, upwelling did not occur; coastal phytoplankton abundances may have been vertically scattered. In addition, all of the biotic and abiotic factors were not significantly different between the OS and IS areas (Figs 5a–f, 6e–h and 10b–e), implying that there was no special or large island effect near Ulleungdo and Dokdo during the study period; both zones were strongly characterized by offshore open water along the U-D line.

4.3 *Vertical physicochemical characteristics along the U-D line*

According to previous studies along the U-D line (Park, 1979; Yang et al., 1991; Gong and Park, 1969; Kim and Chung, 1984; Kim et al., 2007b), although the water mass along the U-D line changes seasonally, the vertical water mass can be divided into five different layers, which are formed by the mixing of the TWC and the NKCC: Type 1: dominant layers of the Tsushima surface

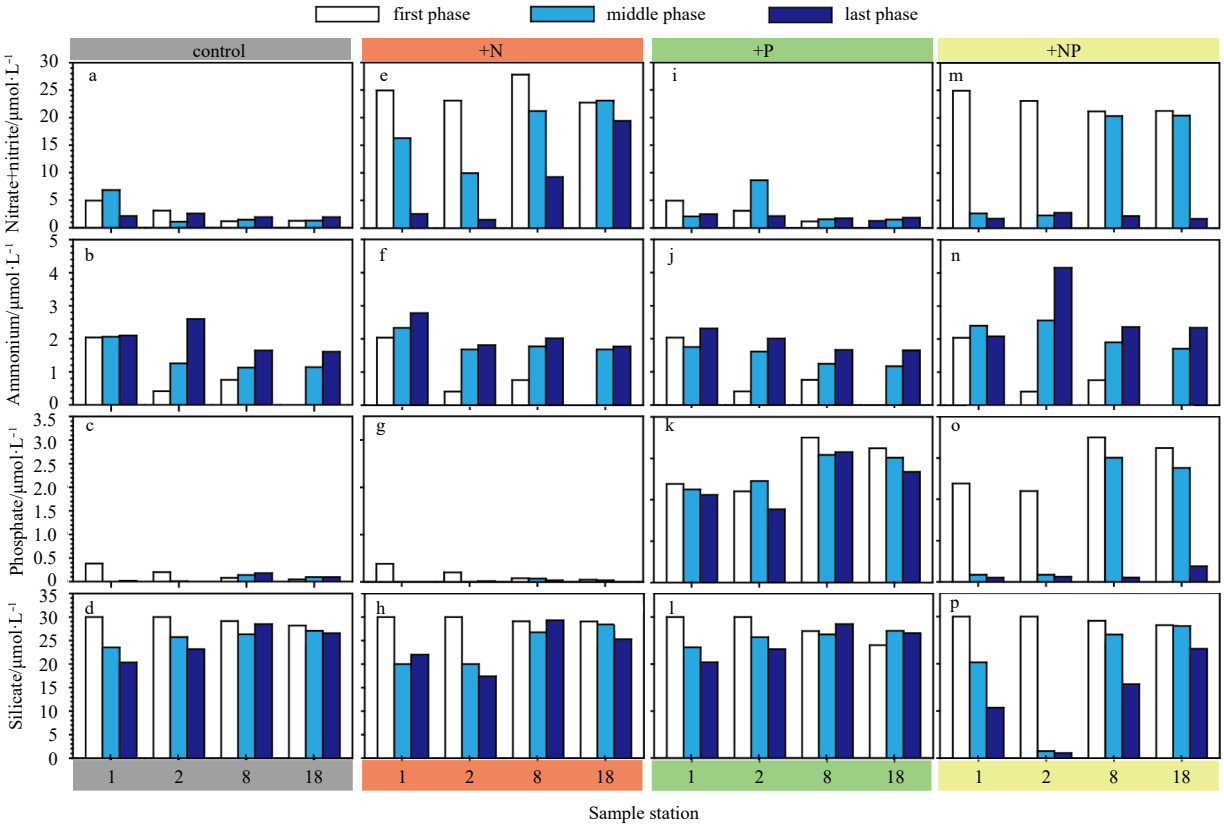

Fig. 12. Changes in nitrate+nitrite (a), ammonium (b), phosphate (c), and silicate (d) concentrations in a bioassay experiment involving no Fe addition. Analyses occurred at the beginning, middle and end of the experiment. Subsamples (10 mL) collected for nutrient analysis were filtered using a disposable syringe filter.

water (<1 m), Type 2: dominant layers of the Tsushima middle water (approximately 20 m), Type 3: water mixing layer with the TWC and NKCC in the upper layer of the thermocline (20–100 m), Type 4: dominant layers of the North Korea Cold Water (100–300 m), and Type 5: dominant layers of the East Sea Proper Water (>300 m). Our vertical profiles showed that the surface layer (0–50 m) in this study area was dominated by the TWC, and the middle layer (50–100 m) had a complex water mass that was mixed with the NKCC (Fig. 8a).

In general, low saline water was maintained in the upper layer and high saline water was maintained in the deeper layer; however, in the present study, relatively high saline water was observed in the upper layer, and low saline water was maintained in the middle and lower layers. From the water density results and based on the relation between water temperature and salinity, the water density was physically dependent on water temperature rather than on salinity in our survey. Therefore, we thought that the oligotrophic high saline water origin of the TWC was dominant in the upper layer, and the expansion of the low saline water origin of the NKCC could extend into the middle and low layers, especially near island stations. The "island effect" was not found in the horizontal analysis; however, the vertical analysis implies that strong northerly winds increased the water depth of the mixing layer, which was caused by the island effect.

In the oceanic environment, the "island effect" can occur, in which variations in the stratification are created by the winds (Gilmartin and Revelante, 1974; Hernández-León, 1991). Along the U-D line, the upper layer of the water column near Ulleungdo (Stas 10–12) was well mixed by a strong windstorm event, and the mixed layer expanded to a depth of 200 m; however, the mixed water mass of the central area (Stas 14–16) remained at a depth of approximately 100 m due to the missing island effect. The mixed water mass deepened gradually to a depth of 150 m near Dokdo (Stas 18–23). In addition, the concentrations of Chl *a* near the island were scattered to the surface from the SCM layer by strong winds. Therefore, if a detailed vertical investigation that includes the wind effect is excluded, the primary production may be underestimated in oceanic environments.

Although the fluorescence values in the waters around Ulleungdo and Dokdo were consistently low throughout the entire water column, the SCM layer in the central area of the UD line clearly appeared at depths of 30–50 m. However, the concentrations of nitrate+nitrite, phosphate and silicate remained low in the surface layer of the U-D line, and their concentrations gradually increased below a depth of 50 m (Fig. 9). Interestingly, phytoplankton biomass in the water around the Ulleungdo and Dokdo was consistently low between 50 m and the surface layer as a result of water mixing; moreover, the nutrient concentrations also remained low to a depth of 50 m, indicating that water mixing was confirmed by both abiotic and biotic evidence. However, the SCM layer was observed in the central area of the U-D line due to the absence of water mixing in the upper layer. As a result, because water mixing caused by the island effect did not significantly appear in the central area of the U-D line, the upper TWC water mass and the lower NKCC hydrodynamic mass were clearly distinguished. Redfield (1958) suggested the Redfield ratio (N:P=16:1) as an important indicator for understanding the properties of aquatic organisms and their environments. In the

present study, the N:P ratio in the upper layers of the SCM exceeded 16 and decreased gradually, although it was nearly constant at 15 to depths of 150–200 m (Figs 9z–d'). Specifically, the phytoplankton biomass gradually decreased, or the SCM layer may have moved deeper in the water column of the euphotic layer because nitrate+nitrite and phosphate were mostly depleted in the upper layer of the SCM. According to Lee et al. (2009), the N:P ratio in the deep region of the East Sea is consistently lower than 16. Lee and Rho (2015) and Baek et al. (2016) also reported that the average N:P ratio below the thermocline layer of the East Sea was relatively low compared to the ratio in the upper euphotic layer, which is similar to our results. However, the reasons explaining the low N:P ratio in the deep layer are unclear, though the biological pump hypothesis, decomposition regulation hypothesis, and seawater circulation hypothesis were discussed by Lee and Rho (2015). Further research is needed to explain the low N:P ratio observed in the deep layer of the East Sea. Here, we confirmed movement of the water mass from the vertical physical, biological and chemical profiles at the U-D line, specifically focusing on the phytoplankton biomass and the nutrient properties after a strong episodic wind storm in oligotrophic offshore waters.

4.4 *Phytoplankton response to nutrient addition*

To evaluate the potential response of phytoplankton to nutrient inputs in the eutrophic-mesotrophic coastal waters (Stas 1 and 2) and the oligotrophic offshore waters (Stas 8 and 18), we carried out the nutrient addition bioassay. High initial nutrient concentrations and phytoplankton abundance were maintained at Stas 1 and 2, though they were low at Stas 8 and 18. Despite sufficient nutrients, phytoplankton growth in the +N and +NP treatments was significantly higher (p<0.05) than that in the control and +P treatment, implying that the additional nutrient-dosing events contributing to coastal areas by river runoff and rainfall can led to accelerated phytoplankton growth, and these additions play an important role in the outbreak of large algal blooms. Diatoms, such as *Chaetoceros* spp., *Leptocylindrus* spp., and *Pseudo-nitzschia* spp., were dominant in the field and grew rapidly in the +N and +NP treatment conditions. Rapid phytoplankton responses to additional nutrient supplies in coastal waters have been reported in the Chesapeake Bay (Fisher et al., 1992) and Louisiana Bay (Smith and Hitchcock, 1994) in USA and in the Gwangyang Bay (Baek et al. 2015), which includes the Seomjin Estuary (Kwon et al., 2002; Lee et al., 2018) in Korea. However, initial low nutrient concentrations and phytoplankton abundances were maintained in oligotrophic offshore waters. Phytoplankton in the nutrient addition experiments responded after 9–10 d, and there was a time lag before growth occurred, even in the +N and +NP treatments, implying that phytoplankton growth may have depended on the initial phytoplankton densities and species composition. In addition, the growth rates of the phytoplankton community remained at approximately one-third the growth rates in the +N and +NP treatments in the coastal area. In our previous bioassay reported by Baek et al. (2018), though similar nutrient addition experiments were performed in an oligotrophic area near Dokdo, phytoplankton growth occurred quickly. At that time, because initial phytoplankton, such as diatoms and Raphidophyta, were dominant during the spring of 2016, the phytoplankton blooms were unlikely to be delayed. However, even though additional nutrients were supplied to the treatments with the initial low phytoplankton abundances, there may still be a time lag before growth responses are observed. Our experiments support that the spring phytoplankton blooms following strong wind events typically occur after a time lag of one week in the East Sea. As a result, the coastal upwelling events in spring can rapidly accelerate the phytoplankton blooms, while downwelling events cannot easily support spring phytoplankton blooms, and thus, these blooms have a time lag even after additional nutrient-dosing events. It is well known that spring phytoplankton blooms following large-scale coastal upwelling in the East Sea are likely to spread out from the coastal area toward the outside of the continental shelf (Hyun et al., 2009; Yoo and Park, 2009). Additionally, the phytoplankton growth response to the +P treatment was not clearly demonstrated, which was similar to the previous study by a combination of field and laboratory experiments (Baek et al., 2018) in the oligotrophic waters of the Ulleungdo and Dokdo. Our bioassays in coastal eutrophic- mesotrophic and offshore oligotrophic areas have demonstrated a favorable phytoplankton growth effect in the +N and +NP treatments, suggesting the phytoplankton growth response was greatly dependent on the initial population density in the oligotrophic area and had a time lag for growth after the nutrient addition. However, further study focusing on the P availability will be required to reveal the cues for spring phytoplankton bloom dynamics in the oligotrophic waters of the Ulleung Basin.

5 Summary and conclusions

In May 2017, the East Sea was strongly influenced by oligotrophic warm currents, and the supplied nutrients were restricted by suppression of upwelling after a strong northwest windstorm event. Overall, the nutrient and Chl *a* concentrations and the phytoplankton biomass were low in the East Sea, including the southeastern Korean coasts and the Ulleung Basin. In the bioassay, little or no prosperity of phytoplankton was observed in the offshore water samples despite the injection of sufficient nutrients. The growth responses of phytoplankton depended on the initial cell density. The bioassay results indicated that both supplying nutrients and introducing enough phytoplankton through the warm currents are critical to maintain the high productivity of the East Sea area. Therefore, an ocean physical, chemical, and biological survey must be performed, including currents and weather information, for a specific and detailed understanding of the production and extinction of primary productivity in this area. In addition, long-term monitoring is needed to evaluate the seasonal fluctuations and to understand the effects of oceanographic events on the primary production in the East Sea.

References

Baek S H, Kim D, Son M, et al. 2015. Seasonal distribution of phytoplankton assemblages and nutrient-enriched bioassays as indicators of nutrient limitation of phytoplankton growth in Gwangyang Bay, Korea. Estuarine, Coastal and Shelf Science, 163: 265–278, doi: 10.1016/j.ecss.2014.12.035

Baek S H, Lee M, Kim Y B. 2016. Growth and community response of phytoplankton by N, P and Fe nutrient addition in around water of Ulleungdo and Dokdo in East Sea. Journal of the Korea Academia-Industrial cooperation Society, 11: 186–195

Baek S H, Lee M, Kim Y B. 2018. Spring phytoplankton community response to an episodic windstorm event in oligotrophic waters offshore from the Ulleungdo and Dokdo islands, Korea. Journal of Sea Research, 132: 1–14, doi: 10.1016/j.seares.2017.11.003

Chung C S, Shim J H, Park Y G, et al. 1989. Primary productivity and nitrogenous nutrient dynamics in the East Sea of Korea. Journal of the Korean Society of Oceanography, 24: 52–61

Fisher T R, Peele E R, Ammerman J W, et al. 1992. Nutrient limitation of phytoplankton in Chesapeake Bay. Marine Ecology Progress Series, 82(1): 51–63

Gilmartin M, Revelante N. 1974. The 'island mass' effect on the

phytoplankton and primary production of the Hawaiian Islands. Journal of Experimental Marine Biology and Ecology, 16(2): 181–204, doi: 10.1016/0022-0981(74)90019-7

Gong Y, Park C K. 1969. On the oceanographical character of the low temperature region in the eastern sea of Korea. Bulletin of Fisheries Research Agency, 4: 69–91

Gong Y, Son S J. 1982. A study of oceanic thermal fronts in the southwestern Japan Sea. Bulletin of Fisheries Research Agency, 28: 25–54

Hernández-León S. 1991. Accumulation of mesozooplankton in a wake area as a causative mechanism of the "island-mass effect". Marine Biology, 109(1): 141–147, doi: 10.1007/BF01320241

Hyun J H, Kim D, Shin C W, et al. 2009. Enhanced phytoplankton and bacterioplankton production coupled to coastal upwelling and an anticyclonic eddy in the Ulleung Basin, East Sea. Aquatic Microbial Ecology, 54: 45–54

Isobe A, Isoda Y. 1997. Circulation in the Japan Basin, the northern part of the Japan Sea. Journal of Oceanography, 53(4): 373–381

Isoda Y, Saitoh S. 1993. The northward intruding eddy along the east coast of Korea. Journal of Oceanography, 49(4): 443–458, doi: 10.1007/BF02234959

Kang Y S, Kim J Y, Kim H G, et al. 2002. Long-term changes in zooplankton and its relationship with squid, *Todarodes pacificus*, catch in Japan/East Sea. Fisheries Oceanography, 11(6): 337–346, doi: 10.1046/j.1365-2419.2002.00211.x

Kang Y S, Choi H C, Lim J H, et al. 2005. Dynamics of the phytoplankton community in the coastal waters of Chuksan harbor, East Sea. Algae, 20(4): 345–352, doi: 10.4490/ALGAE.2005.20.4.345

Kim K, Chung J Y. 1984. On the salinity-minimum and dissolved oxygen-maximum layer in the East Sea (Sea of Japan). In: Elsevier Oceanography Series. Amsterdam: Elsevier, 55–65

Kim D S, Kim K H, Shim J H, et al. 2007a. The effect of anticyclonic eddy on nutrients and chlorophyll during spring and summer in the Ulleung Basin, East Sea. The Sea, 12(4): 280–286

Kim J H, Wang P B, Park B S, et al. 2018. Revealing the distinct habitat ranges and hybrid zone of genetic sub-populations within *Pseudo-nitzschia pungens* (Bacillariophyceae) in the West Pacific area. Harmful Algae, 73: 72–83, doi: 10.1016/j.hal.2018.01.007

Kim D, Yang E J, Kim K H, et al. 2012. Impact of an anticyclonic eddy on the summer nutrient and chlorophyll a distributions in the Ulleung Basin, East Sea (Japan Sea). ICES Journal of Marine Science, 69(1): 23–29, doi: 10.1093/icesjms/fsr178

Kim H C, Yoo S J, Oh I S. 2007b. Relationship between phytoplankton bloom and wind stress in the sub-polar frontal area of the Japan/East Sea. Journal of Marine Systems, 67(3–4): 205–216, doi: 10.1016/j.jmarsys.2006.05.016

Kim C H, Yoon J H. 1999. A numerical modeling of the upper and the intermediate layer circulation in the East Sea. Journal of Oceanography, 55(2): 327–345, doi: 10.1023/A:1007837212219

Kwak J H, Hwang J, Choy E J, et al. 2013. High primary productivity and f-ratio in summer in the Ulleung basin of the East/Japan Sea. Deep Sea Research Part I: Oceanographic Research Papers, 79: 74–85, doi: 10.1016/j.dsr.2013.05.011

Kwon K Y, Moon C H, Kang C K, et al. 2002. Distribution of particulate organic matters along the salinity gradients in the Seomjin River estuary. Korean Journal of Fisheries and Aquatic Science, 35(1): 86–96, doi: 10.5657/kfas.2002.35.1.086

Lee J. 1983. Variations of sea level and sea surface temperature associated with wind-induced upwelling in the southeast coast of Korea in summer. Journal of the Korean Society of Oceanography, 18(2): 149–160

Lee J B, Han M S, Yang H S. 1998. The ecosystem of the southern coastal waters of the East Sea, Korea: I. Phytoplankton community structure and primary productivity in September, 1994. Korean Journal of Fisheries and Aquatic Science, 31(1): 45–55

Lee J Y, Kang D J, Kim I N, et al. 2009. Spatial and temporal variability in the pelagic ecosystem of the East Sea (Sea of Japan): a review. Journal of Marine Systems, 78(2): 288–300, doi: 10.1016/j.jmarsys.2009.02.013

Lee J C, Na J Y. 1985. Structure of upwelling off the southeast coast of Korea. Journal of the Korean Society of Oceanography, 20: 6–19

Lee M, Park B S, Baek S H. 2018. Tidal influences on biotic and abiotic factors in the Seomjin River Estuary and Gwangyang Bay, Korea. Estuaries and Coasts, 41(7): 1977–1993, doi: 10.1007/s12237-018-0404-9

Lee T, Rho T K. 2015. Seawater N/P ratio of the East Sea. The Sea, 20(4): 199–205, doi: 10.7850/jkso.2015.20.4.199

Liu G M, Chai F. 2009. Seasonal and interannual variation of physical and biological processes during 1994–2001 in the Sea of Japan/East Sea: a three-dimensional physical-biogeochemical modeling study. Journal of Marine Systems, 78(2): 265–277, doi: 10.1016/j.jmarsys.2009.02.011

Martin S, Kawase M. 1998. The southern flux of sea ice in the Tatarskiy Strait, Japan Sea and the generation of the Liman Current. Journal of Marine Research, 56(1): 141–155, doi: 10.1357/002224098321836145

Mooers C N K, Bang I, Sandoval F J. 2005. Comparisons between observations and numerical simulations of Japan (East) Sea flow and mass fields in 1999 through 2001. Deep Sea Research Part II: Topical Studies in Oceanography, 52(11–13): 1639–1661, doi: 10.1016/j.dsr2.2004.10.003

Moon C H, Yang S R, Yang H S, et al. 1998. Regeneration processes of nutrients in the polar front area of the last sea: IV. Chlorophyll a distribution, new production and the vertical diffusion of nitrate. Korean Journal of Fisheries and Aquatic Science, 31(2): 259–266

Oh H J, Suh Y S, Heo S. 2004. The relationship between phytoplankton distribution and environmental conditions of the upwelling cold water in the eastern coast of the Korean peninsula. Journal of the Korean Association of Geographic Information Studies, 7: 166–173

Ohshima K I. 1994. The flow system in the Japan Sea caused by a sea level difference through shallow straits. Journal of Geophysical Research, 99(C5): 9925–9940, doi: 10.1029/94JC00170

Park C K. 1979. On the distribution of dissolved oxygen off the east coast of Korea. Journal of the Korean Society of Oceanography, 14(2): 67–70

Park B S, Kim J H, Kim J H, et al. 2018. Intraspecific bloom succession in the harmful dinoflagellate *Cochlodinium polykrikoides* (Dinophyceae) extended the blooming period in Korean coastal waters in 2009. Harmful Algae, 71: 78–88, doi: 10.1016/j.hal.2017.12.004

Parsons T R. 2013. A Manual of Chemical & Biological Methods for Seawater Analysis. New York: Elsevier

Redfield A C. 1958. The biological control of chemical factors in the environment. American Scientist, 46: 205–221

Ryan J P, Polito P S, Strutton P G, et al. 2002. Unusual large-scale phytoplankton blooms in the equatorial Pacific. Progress in Oceanography, 55(3–4): 263–285, doi: 10.1016/S0079-6611(02)00137-4

Smith S M, Hitchcock G L. 1994. Nutrient enrichments and phytoplankton growth in the surface waters of the Louisiana Bight. Estuaries, 17(4): 740–753, doi: 10.2307/1352744

Smith V H, Tilman G D, Nekola J C. 1999. Eutrophication: impacts of excess nutrient inputs on freshwater, marine, and terrestrial ecosystems. Environmental Pollution, 100(1–3): 179–196, doi: 10.1016/S0269-7491(99)00091-3

Sournia A. 1978. Phytoplankton Manual: Monographs on Oceanographic Methodology. Vol 6. Paris: UNESCO

Tsuchiya K, Kuwahara V S, Yoshiki T, et al. 2014. Phytoplankton community response and succession in relation to typhoon passages in the coastal waters of Japan. Journal of Plankton Research, 36(2): 424–438, doi: 10.1093/plankt/fbt127

Wasmund N, Andrushaitis A, Łysiak-Pastuszak E, et al. 2001. Trophic status of the south-eastern Baltic Sea: a comparison of coastal and open areas. Estuarine, Coastal and Shelf Science, 53(6): 849–864, doi: 10.1006/ecss.2001.0828

Yang H S, Kim S S, Kang C G, et al. 1991. A study on sea water and ocean current in the sea adjacent to Korea Peninsula-III. Chemical characteristics of water masses in the polar front area of the central Korean East Sea. Korean Journal of Fisheries and

Aquatic Science, 24(3): 185–192

Yoo S, Park J. 2009. Why is the southwest the most productive region of the East Sea/Sea of Japan?. Journal of Marine Systems, 78(2): 301–315, doi: 10.1016/j.jmarsys.2009.02.014

Zhang C I, Lee J B, Kim S, et al. 2000. Climatic regime shifts and their impacts on marine ecosystem and fisheries resources in Korean waters. Progress in Oceanography, 47(2–4): 171–190, doi: 10.1016/S0079-6611(00)00035-5

Zhang J, Liu S M, Ren J L, et al. 2007. Nutrient gradients from the eutrophic Changjiang (Yangtze River) Estuary to the oligotrophic Kuroshio waters and re-evaluation of budgets for the East China Sea Shelf. Progress in Oceanography, 74(4): 449–478, doi: 10.1016/j.pocean.2007.04.019

Zhao Hui, Tang Danling, Wang Yuqing. 2008. Comparison of phytoplankton blooms triggered by two typhoons with different intensities and translation speeds in the South China Sea. Marine Ecology Progress Series, 365: 57–65, doi: 10.3354/meps07488

Supplementary information:

Table S1. Average wind speed, maximum wind speed, and wind direction in May for the ten recent years

Fig. S1. Short-term variability in Chl *a* concentration processed by GDPS in the East Sea from COMS/GOCI on May 19 (a), May 27 (b) and June 5 (d) in 2017.

The supplementary information is available online at https://doi.org/10.1007/s13131-020-1545-9. The supplementary information is published as submitted, without typesetting or editing. The responsibility for scientific accuracy and content remains entirely with the authors.